Fault-Tolerant Control of a Blade-pitch Wind Turbine With Inverter-fed Generator

V. Lešić, M. Vašak, N. Perić
Faculty of Electrical Engineering and Computing
University of Zagreb
Zagreb, Croatia
e-mail: vinko.lesic@fer.hr

T. Wolbank
Faculty of Electrical Engineering and Information Technology
Vienna University of Technology
Vienna, Austria

G. Joksimović
Faculty of Electrical Engineering
University of Montenegro
Podgorica, Montenegro

***Abstract*—A fact is that wind energy is both green and expensive energy. In order to increase its economic competence, wind turbine faults should be reduced and prevented. In wind turbines faults most commonly occur in the gearbox and in the generator system components like power converter or generator electromechanical parts. This paper proposes a fault-tolerant control strategy for variable-speed variable-pitch wind turbines in case of identified and characterized generator electromechanical faults like broken rotor bar or winding inter-turn fault. In particular we propose an upgrade of the torque control loop with flux-angle-based torque modulation. Usage of pitch controller in the low wind speed region is also proposed to intentionally reduce power capture in order to avoid or to postpone the system fault development. Presented fault-tolerant control techniques are developed considering their easy implementation and installation in available control systems of existing wind turbines to extend their life cycle and energy production. Simulation results for the case of 700 kW direct-drive wind turbine and the identified stator winding fault are presented.**

I. Introduction

Due to global warming and climate changes, renewable energy sources and green energy have considerable impact on today's economy. Wind energy is the fastest-growing renewable energy source. Compared however with fossil fuel based power systems, wind energy is considered to be a low power quality unreliable source with low conversion efficiency, which results in an expensive energy system. Therefore, the main goal is to develop effective and efficient renewable energy systems and to achieve minimization of the cost and maintenance of the corresponding installation at the same time.

To keep the efficiency of energy conversion processes in wind turbines at or near their optimum values all system components have to be continuously monitored. If there is some kind of fault detected in the system, wind turbines today have a safety protocol which rotates its blades at 90° pitch angle and halts the turbine rotation by reducing the aerodynamic torque to zero and behaving as an aerodynamic break. Energy production therefore also drops to zero.

Many of these faults can be detected through a monitoring system long before they become fully developed and trigger the shut-down protocol. Once noticed, the development of the fault should be slowed down by a fault-tolerant control system that extends the life and operation time of expensive turbine components and sustains the energy production.

Focus of this paper is, therefore, to research and develop a fault-tolerant extension of the wind turbine control system for the case of generator electromechanical faults, which are besides gearbox and power converters faults the most common in wind turbine systems [1]. In case of identified faults, it adapts control actions through a fast control loop for flux-angle-based modulation of the generator torque, and through a slow control loop that ensures the generator placement at a point of its speed-torque plane where it is possible to:

- enable the fast loop to perform correctly,
- protect the generator and other wind turbine components by stopping the fault further development,
- keep the electrical energy production optimal under emergency circumstances.

This paper is organized as follows. Wind turbine electrical subsystem with different generator types is described in Section II. Some of the basic control strategies for a variable-speed variable-pitch wind turbine are presented in Section III along with its normal operating maps. In Section IV, a fault-tolerant approach and control algorithm is proposed and described to enable wind turbine operation in emergency state. Section V provides MATLAB/Simulink simulation results obtained with the proposed fault-tolerant control startegy.

II. Electrical subsystem

Wind turbine in principle consists of a three-blade aerodynamic system mounted on a hub, of a nacelle and of a tower. Inside the nacelle there is a drivetrain with optional gearbox and electrical subsystem with a generator and an electronic converter. There are several types of generators used in wind turbines: doubly-fed induction generator (DFIG) with a wound rotor connected to the grid through slip rings and electronic converter (EC), squirrel-cage induction generator (SCIG) with an EC connected to the stator (Fig. 1) and a direct-drive synchronous generator (SG) coupled to the grid through an EC and with rotor slip-rings for the excitation voltage. A lot of effort is currently put into developing large-scale synchronous generators with permanent magnets.

978-1-4244-9311-1/11/$26.00 ©2011 IEEE

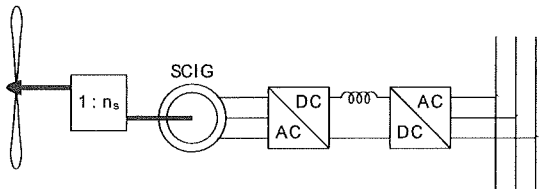

Fig. 1. Stator-controlled squirrel cage induction generator.

Fault-tolerant control proposed in this paper can be applied to any of listed wind turbine electrical subsystems, assuming that the generator tracks the given torque reference with certain dynamics. In the following we thus consider the generator torque tracking system as a first-order lag system.

Every type of generator has its own way of speed control and it can be used to shift operating points in the generator x-axis of speed-torque plane. By using pitch control of a wind turbine aerodynamic torque can be also displaced in the y-axis. This gives the control system the ability to move the operating point with two degrees of freedom in the speed-torque plane.

III. Control objectives

Taking into consideration both physical and economic constraints, the optimum point to which the wind power capture will rise is chosen, which determines the wind turbine rated power (full line in Figure 2). Thus, operating map of the turbine is parted into a low wind speed region (region I), where all the available wind power is fully captured and high wind speed region (region II) where the power output is maintained constant while reducing the aerodynamic torque to the rated value and keeping generator speed at the rated value.

The ability of a wind turbine to capture wind energy is expressed through a power coefficient C_P which is defined as the ratio of extracted power P_r to wind power P_V:

$$C_P = \frac{P_r}{P_V}. \tag{1}$$

The maximum value of C_P, known as Betz limit, is $C_{Pmax} = \frac{16}{27} = 0.593$. It defines the maximum theoretical capability of wind power capture. The real power coefficient of modern commercial wind turbines reaches values of about 0.48 [2]. Power coefficient data is usually given as a function of the tip-speed-ratio λ and pitch angle β (Fig. 3). Turbine power and torque are given by [3]

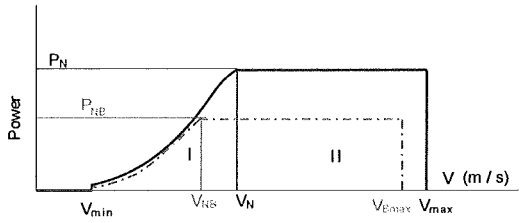

Fig. 2. Ideal power curve with maximum P_N and power curve due to developed fault with maximum P_{NB}.

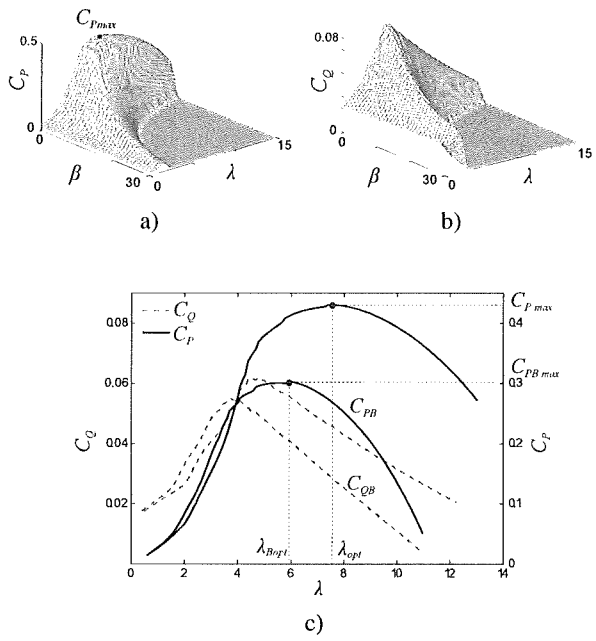

Fig. 3. Power a) and torque b) coefficients for an exemplary 700kW variable-pitch turbine. Fig. c) is for optimal β_0 in low wind speed region (C_P, C_Q) and for $\beta = 10°$ (C_{PB}, C_{QB}).

$$P_r = C_P(\lambda, \beta) P_V = \frac{1}{2}\rho R^2 \pi C_P(\lambda, \beta) V^3, \tag{2}$$

$$T_r = \frac{P_r}{\omega} = \frac{1}{2}\rho R^3 \pi C_Q(\lambda, \beta) V^2, \tag{3}$$

where $C_Q = C_P/\lambda$, ρ, R, V and ω are torque coefficient, air density, radius of aerodynamic disk, wind speed and the angular speed of blades, respectively, and $\lambda = \frac{\omega R}{V}$.

A. Variable-speed control

Since the goal is to maximize the output power in low wind speed region, wind turbine must operate in the area where the power coefficient C_P is at its maximum value (or near it). This is achieved by maintaining λ and β on the values that ensure $C_P = C_{Pmax}$ [2]-[6], see Fig. 3. To achieve the operating point in which λ is optimal, the generator torque and consequently the aerodynamic torque is determined by

$$T_{gref} = \frac{1}{2\lambda_{opt}^3 n_s^3}\rho\pi R^5 C_{Pmax}\omega_g^2 = K_\lambda \omega_g^2, \tag{4}$$

where n_s is the gearbox ratio. This way the wind turbine operating points in low wind speed region are located at the maximum output power curve, called C_{Pmax} locus (BC path on Fig. 5). This $T_{gref} = K_\lambda \omega_g^2$ torque controller (Fig. 4) can be easily realized using a simple look-up table.

B. Pitch control

Above designated rated wind speed, available wind power is higher than the generator rated power and it rises rapidly

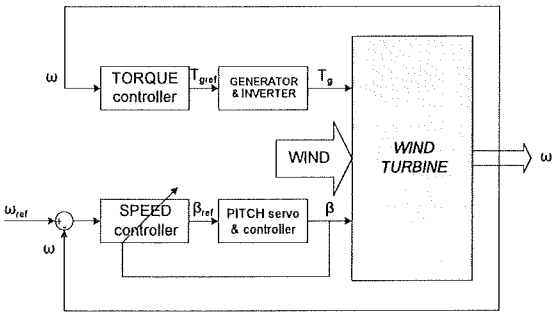

Fig. 4. Control system of a variable-speed variable-pitch wind turbine.

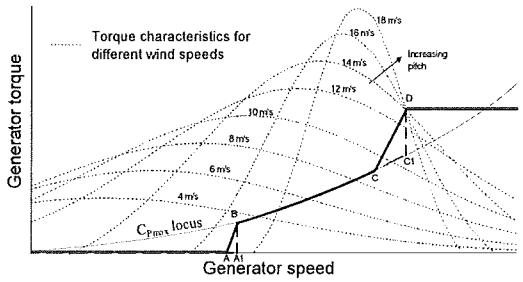

Fig. 5. Control strategy of a variable-speed wind turbine [4].

along with the wind speed (see (2)). Therefore, the task of the control system is to maintain output power of the wind turbine constant. It can be done by reducing the aerodynamic torque and angular speed of blades by rotating them along their longitudinal axis (pitching). Consequently, power captured from the wind is reduced.

Control system (Fig. 4) is usually designed in a cascade structure with inner loop representing the servo drive position control of blades to the reference pitch angle β_{ref} defined by the outer speed control loop. Outer loop controls the rotational speed of the wind turbine and sets it to the reference (rated) value. A PI or proportional-integral-derivative (PID) controller with gain-scheduling technique is often satisfactory for pitch control.

C. Switching between torque and pitch control

Following the C_{Pmax} locus curve, wind turbine usually reaches its rated angular speed before it reaches its rated torque. It is then desirable to increase the torque and power without any further speed increase. This is achieved by improving the torque control loop with a closed-loop controller that maintains the torque on its rated value ($A1BC1D$ characteristic in Fig. 5). Usually smooth transition between the torque control and pitch control operating regimes of the wind turbine is enforced by deviating from the optimal power curve on edges of the low wind speed region [4], characteristic $ABCD$ in Fig. 5.

IV. Fault-Tolerant Control

In previous sections some of the most common and reliable wind turbine control strategies are described. This section extends them to propose a fault-tolerant control approach designed to protect wind turbine components by disabling generator fault further development and to keep energy production optimal in emergency state. Common faults of an electric machine are stator winding inter-turn short circuit, rotor bar defect in case of squirrel-cage induction machines and rotor eccentricity. These faults may lead to overheating or breaking of the defected component and thus possibly to a catastrophic fault. Consequently, it triggers the safety procedure and results in a wind turbine shut-down. Whole repair process requires immense amounts of money and the situation is even worse for off-shore wind turbines. So, from this aspect, it is an interesting idea to reduce voltage or current stress on the faulty part of the generator as it operates and to anticipate such fault-tolerant behavior in overall torque-speed control of the turbine. This way, the fault development will be evaded or postponed while at the same time it will be possible to optimize the energy production in the non-healthy generator state. This increases wind turbine's total energy output and consequently its economic value.

In case of a machine fault (like damaged rotor bar or stator winding fault), magnetic flux of the machine only on a small part of its path as it moves along the circumference affects the damaged component. That part of the magnetic flux path is denoted with $\Delta\theta = \theta_2 - \theta_1$, see Fig. 6. Our primary goal is to reduce the electrical stress reflected through the generator torque in that angle span to the maximum allowed safety value T_{gf}. The value T_{gf} is determined based on fault identification through machine fault monitoring and characterization techniques, together with flux angles θ_1 and θ_2 [7]. For the case of identified rotor bar damage a fault identification procedure directly outputs the safety torque value T_{gf} together with the location (values θ_1 and θ_2) in the rotor magnetic flux frame to reduce mechanical stress on the damaged rotor bar. For the case of identified stator winding inter-turn fault, a fault identification procedure localizes the damaged part in the stator magnetic flux frame and outputs the maximum allowed machine flux time derivative on the damaged part which can be transferred to the maximum safety torque allowed with respect to the generator speed.

Instead of torque reduction in the whole rotational period as a reaction to the fault, a fast control loop is proposed to reduce torque only in the $\Delta\theta$ section of the flux rotation path. Flux in the air-gap, and consequently torque, is therefore modulated, based on the machine flux angular position with respect to the

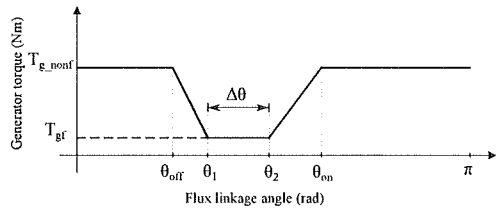

Fig. 6. Torque modulation due to a fault condition.

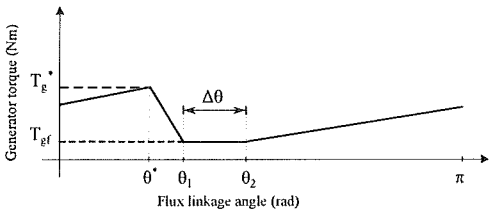

Fig. 7. Torque modulation due to a fault condition when T_{g_nonf} cannot be restored.

damaged part. In case of e.g. induction generators, this method is applied using a field-oriented control (FOC) technique.

Torque modulation is shown in Fig. 6. When the flux in angle θ approaches the angle span $\Delta\theta$, the torque is reduced to the maximum allowed value T_{gf} defined with a fault condition and, possibly, current generator speed. After the flux passes it, torque is restored to the right selected value T_{g_nonf}. The value of T_{g_nonf} is determined such that the average machine torque is maintained on the optimal level, taking into account the machine constraints. Procedure is then periodically executed, with electrical angle period equal π, since the flux influences the faulty part with its north and south pole in each turn. Due to the finite bandwidth of the torque control loop, it is necessary to start reducing the torque prior to reaching the flux angle θ_1, while the torque is restored to the value T_{g_nonf} at the electrical angle θ_{on} after passing θ_2.

Torque transitions between steady-state operating areas are simplified and presented as linear characteristics that correspond to maximum available torque decrease/increase rate determined by maximum possible currents decrease/increase rates, i.e. by the power converter DC link constraints. Considering more realistic torque changes which would be a mix of linear and exponential functions can be also handled but is in the following presentation omitted to facilitate the mathematical treatment of the proposed method. Fig. 6 also shows that reducing the torque takes less time than restoring it. This is due to the back-electromotive force which opposes the current and thereby aggravates torque restoration. Available torque rates for generator torque decrease and increase are denoted with $\dot{T}_{g-}(\omega_g)$ and $\dot{T}_{g+}(\omega_g)$, respectively.

In the following we derive the fault-tolerant control strategy for the synchronous machine stator fault due to stator winding inter-turn fault, but similar strategy can be also derived for a faulty asynchronous machine, either for the rotor bar defect or for the inter-turn winding fault on the stator. For easier mathematical treatment we assume constant value of T_{gf}, although for this type of fault there exists an inverse-proportional relation between T_{gf} and electrical speed. Since the generator electrical speed in case of synchronous machine is defined as

$$\omega_e = p\omega_g = \frac{\Delta\theta}{\Delta t} \tag{5}$$

and duration of the torque decrease transient as

$$\Delta t_{off} = \frac{T_{g\_nonf} - T_{gf}}{\dot{T}_{g-}(\omega_g)}, \tag{6}$$

by combining these two relations the following is obtained:

$$\frac{\theta_1 - \theta_{off}}{p\omega_g} = \frac{T_{g\_nonf} - T_{gf}}{\dot{T}_{g-}(\omega_g)}. \tag{7}$$

Finally, θ_{off} can be derived from (7):

$$\theta_{off} = \theta_1 - p\omega_g \frac{T_{g\_nonf} - T_{gf}}{\dot{T}_{g-}(\omega_g)}. \tag{8}$$

In the same way, θ_{on} is obtained as

$$\theta_{on} = \theta_2 + p\omega_g \frac{T_{g\_nonf} - T_{gf}}{\dot{T}_{g+}(\omega_g)}. \tag{9}$$

If the torque value T_{g_nonf} can be restored at some angle, then

$$\theta_{on} - \theta_{off} \leqslant \pi. \tag{10}$$

Putting (8) and (9) into (10), the following is obtained for condition (10):

$$p\omega_g(T_{g\_nonf} - T_{gf}) \left[\frac{1}{\dot{T}_{g+}(\omega_g)} + \frac{1}{\dot{T}_{g-}(\omega_g)} \right] \leqslant \pi - \Delta\theta. \tag{11}$$

Because of large inertia of the whole drivetrain, generator and blade system, these torque oscillations are barely noticeable on the speed transient, such that the speed is affected by the mean torque value:

$$T_{av} = \frac{1}{\pi} \int_0^{\pi} T_g \mathrm{d}\theta. \tag{12}$$

Mean value of the generator torque from Fig. 6 is then given by

$$T_{av} = T_{g\_nonf} \frac{\pi - (\theta_{on} - \theta_{off})}{\pi} + \frac{T_{gf} + T_{g\_nonf}}{2} \cdot \frac{\theta_1 - \theta_{off}}{\pi} + T_{gf} \frac{\theta_2 - \theta_1}{\pi} + \frac{T_{gf} + T_{g\_nonf}}{2} \frac{\theta_{on} - \theta_2}{\pi}. \tag{13}$$

Equation (10) (or (11)) is not satisfied if the speed ω_g is large enough (or if there is a large rotor path under fault influence). In that case the torque modulation is given with Fig. 7 and peak torque T_g^* is attained at angle θ^*:

$$\theta_2 - \pi + p\omega_g \frac{T_g^* - T_{gf}}{\dot{T}_{g+}(\omega_g)} = \theta_1 - p\omega_g \frac{T_g^* - T_{gf}}{\dot{T}_{g-}(\omega_g)}. \tag{14}$$

Values T_g^* and θ^* can be expressed as:

$$T_g^* = T_{gf} + \frac{\pi - \Delta\theta}{p\omega_g \left(\frac{1}{\dot{T}_{g+}(\omega_g)} + \frac{1}{\dot{T}_{g-}(\omega_g)} \right)}, \tag{15}$$

$$\theta^* = \theta_1 - \frac{\pi - \Delta\theta}{1 + \frac{\dot{T}_{g-}(\omega_g)}{\dot{T}_{g+}(\omega_g)}}. \tag{16}$$

Mean value of the generator torque from Fig. 7 (i.e. in case when (10) is not satisfied) is now given by

$$T_{av} = T_{gf} \frac{\theta_2 - \theta_1}{\pi} + \frac{T_{gf} + T_g^*}{2} \frac{\theta^* + \pi - \theta_2}{\pi} + \frac{T_{gf} + T_g^*}{2} \frac{\theta_1 - \theta^*}{\pi}. \tag{17}$$

Concludingly, if (11) is fulfilled, the resulting average torque is given with (13); if not, then the resulting average torque is given with (17). On the boundary, i.e. for equality in (10) or (11), both (13) and (17) give the same torque T_{av}, such that $T_{av}(\omega_g)$ is continuous. The maximum available torque T_{g_nonf} is the nominal generator torque T_{gn}. Replacing T_{g_nonf} in (13) with the nominal generator torque T_{gn} gives the maximum available average torque under fault characterized with $\Delta\theta$ and T_{gf}. Replacing T_{g_nonf} with T_{gn} in (11) will result in speed ω_g^* up to which it is possible to restore the nominal torque in the generator in case of the considered fault. Above ω_g^*, (17) holds for the average torque. Fig. 8 shows an exemplary graph of available speed-torque points under machine fault, where the upper limit is based on relations (11), (13) and (17) with $T_{g\_nonf} = T_{gn}$. Dashed area denotes all available average generator torque values that can be achieved for certain generator speed.

From Fig. 8 it follows that up to the speed ω_{g1} it is possible to control the wind turbine in the faulty case without sacrificing power production. However, from that speed onwards it will be necessary to use blades pitching in order to limit the aerodynamic torque (e.g., C_{PB} and C_{QB} in Fig. 3) and to keep the power production below optimal in order to suppress the fault from spreading. The speed control loop is modified such that instead of reference ω_n the reference ω_1 (in case of gearbox, $\omega_1 = \omega_{g1}/n_s$) is selected. This activates pitch control once the right edge of the feasible-under-fault optimal torque characteristics is reached. The optimal power point on $T_{av}(\omega_g)$, which is always on the upper edge of the dashed area, may deviate from this point and thus further improvements in power production outside the point $(\omega_{g1}, T_{av}(\omega_{g1}))$ may be obtained by using maximum power tracking control along the curve of maximum T_{av} in the speed span $[\omega_{g1}, \omega_{gn}]$. The interventions in classical wind turbine control that ensure fault-tolerant control are given in Fig. 9. Algorithms of the slow and the fast fault-tolerant control loops are given in the sequel.

1) Fault-tolerant control algorithm, slow loop:

I. Compute T_{g_nonf} from (8), (9) and (13) such that $T_{av}(\omega_g) = T'_{gref}$; if $T_{g\_nonf} > T_{gn}$, set $T_{g\_nonf} = T_{gn}$;

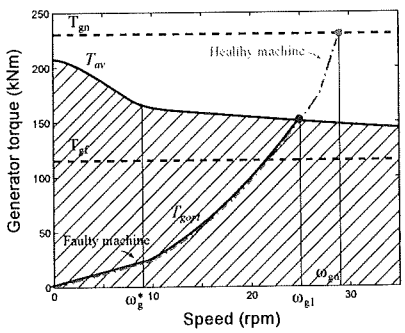

Fig. 8. Available torque-speed generator operating points under fault condition (shaded area). Full line is the achievable part of the wind turbine torque-speed curve under faulty condition. Dash-dot line is the healthy machine curve.

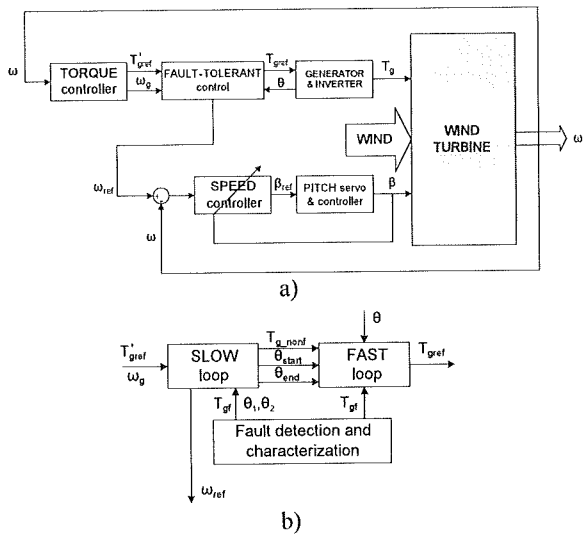

Fig. 9. a) Control system of wind turbine with fault-tolerant control strategy. b) Enlarged fault-tolerant control block.

II. If (11) is fulfilled set $\theta_{start} = \theta_{off} \bmod \pi$ else compute θ^* from (16) and set $\theta_{start} = \theta^* \bmod \pi$ and $T_{g\_nonf} = T_{gn}$; set $\theta_{end} = \theta_2$;

III. Compute ω_{g1} as a speed coordinate of the intersection point of $T_{av}(\omega_g)$ and of the normal wind turbine torque controller characteristics, compute $\omega_1 = \omega_{g1}/n_s$ and set $\omega_{ref} = \omega_1$.

2) Fault-tolerant control algorithm, fast loop:

I. On the positive edge of logical condition $\theta > \theta_{end}$ set $T_{gref} = T_{g\_nonf}$. On the positive edge of the logical condition $\theta > \theta_{start}$ set $T_{gref} = T_{gf}$.

V. Simulation Results

This section provides simulation results for a 700 kW MATLAB/Simulink variable-speed variable-pitch wind turbine model. The direct-drive 60-pole synchronous generator torque control system is modelled as a first-order lag system with time constant $\tau_{gen} = 0.02$ s. Turbine parameters are: $C_{Pmax} = 0.4745$, $R = 25$ m, $\lambda_{opt} = 7.4$, $\omega_n = 29$ rpm and $T_{gn} = 230.5$ kNm. Fault is simulated between flux angles $\theta_1 = \frac{\pi}{2}$ and $\theta_2 = \frac{\pi}{2} + \frac{\pi}{5}$, with $T_{gf} = 0.5\,T_{gn}$ and presented fault-tolerant control algorithm is applied. Results in Fig. 10 show how the wind turbine behaves in healthy and faulty condition for a linear change of wind speed through the entire wind turbine operating area.

Fig. 11 shows the fault-tolerant control system reaction to the fault that is identified in $t = 35$ s for the case when the average generator torque under fault $T_{av}(\omega_g)$ can be equal to the required torque T'_{gref} for the incurred speed ω_g, i.e. the optimum speed-torque point is in the dashed area of Fig. 8 for the occurred fault.

Fig. 12 shows the fault-tolerant control system reaction to the fault identified in $t = 35$ s for the case when the incurred healthy machine speed-torque operating point falls out of the

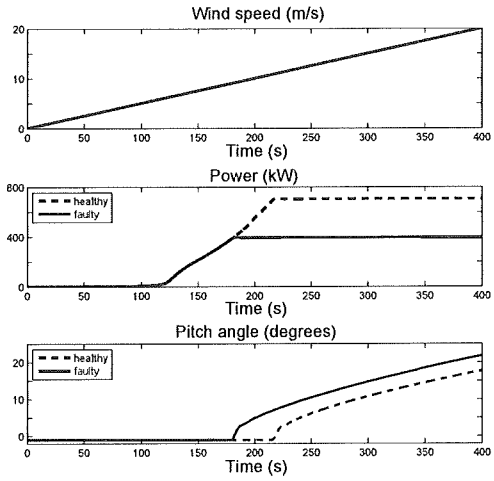

Fig. 10. Wind turbine output power and pitch angle for healthy and faulty conditions.

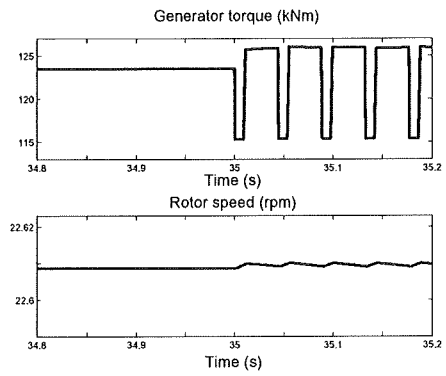

Fig. 11. Generator torque modulation and wind turbine speed when the operating point of healthy machine is feasible under fault. Fault occurs at 35 s.

dashed area of Fig. 8. In this case blade pitching is used in the faulty condition to bring the speed-torque operating point into $(\omega_{g1}, T_{av}(\omega_{g1}))$.

VI. Conclusions

In this paper we propose a fault-tolerant control scheme for blade-pitch wind turbines with an inverter-fed generator. We focus on generator faults that can be well characterized with machine flux path areas where the generator torque should be limited to prevent fault propagation and with the maximum safety torque value in that path areas. We propose a simple extension of the classical two-loop control structure of blade-pitch wind turbines which ensures that the fault is fully respected in operation and that power delivery under fault is deteriorated as less as possible compared to healthy machine conditions.

Acknowledgement

This work has been supported by the European Commission and the Republic of Croatia under grant FP7-SEE-ERA.net PLUS ERA 80/01.

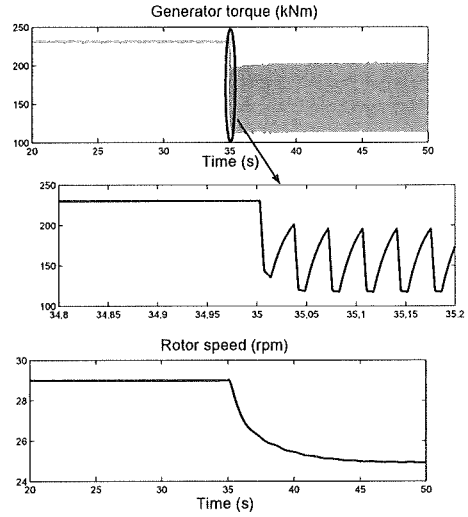

Fig. 12. Generator torque modulation and wind turbine speed when the operating point of healthy machine is not feasible under fault. Fault occurs at 35 s.

References

[1] Z. Daneshi-Far, G. A. Capolino, H. Henao, "Review of Failures and Condition Monitoring in Wind Turbine Generators", *XIX International Conference on Electrical Machines - ICEM 2010*, September 2010.

[2] M. Jelavić, N. Perić, I. Petrović, M. Kajari and S. Car, "Wind turbine control system", *Proc. of the 7th Symposium on Power System Management, HO CIGRE*, November 2006, pp. 196-201.

[3] F. D. Bianchi, H. De Battista and R. J. Mantz, *Wind Turbine Control Systems - Principles, Modelling and Gain Scheduling Design.*, London, England: Springer, ISBN 1-84628-492-9, 2007.

[4] T. Burton, D. Sharpe, N. Jenkins and E. Bossanyi *Wind Energy Handbook*, England: John Wiley & Sons, ISBN 0-471-48997-2, 2001.

[5] K. E. Johnson, L. Y. Pao, M. J. Balas and L. J. Fingersh: Control of Variable-Speed Wind Turbines, *IEEE Control Systems Magazine*, 1066-033x, June 2006, pp. 70-81.

[6] M. Jelavić, N. Perić, and I. Petrović, "Identification of Wind Turbine Model for Controller Design", in *Proc. of the 12th International Power Electronics and Motion Control Conf. EPE - PEMC 2006*, Aug. 30 -Sep. 1, 2006, pp. 1608-1613.,

[7] G. Stojičić, P. Nussbaumer, G. Joksimović, M. Vašak, N. Perić and T. M. Wolbank, "Precise Separation of Inherent Induction Machine Asymmetries from Rotor Bar Fault Indicator", *8th IEEE International Symposium on Diagnostics for Electrical Machines, Power Electronics & Drives, SDEMPED*, 2011.

[8] M. P. Kazmierkowski, F. Blaabjerg and R. Krishnan, *Control in Power Electronics - Selected Problems*, San Diego, California: Academic Press, An imprint of Elsevier Science, ISBN 0-12-402772-5, 2002.

[9] M. Jelavić, N. Perić, I. Petrović, S. Car and M. Madjerčić, "Design of a Wind Turbine Pitch Controller for Loads and Fatigue Reduction", *Proc. of the European Wind Energy Conference & Exhibition - EWEC 2007*, May 2007.

[10] F. Blaabjerg, F. Iov, R. Teodorescu and Z. Chen. "Power Electronics in Renewable Energy Systems" *Proc. of the 12th International Power Electronics and Motion Control Conf. (EPE-PEMC 2006)*, 2006.

[11] J. Lewis and C. Muller, "A Direct Drive Wind Turbine HTS Generator" *IEEE Power Engineering Society General Meeting*, 2007.

[12] P. Novak, T. Ekelund, I. Jovik and B. Schmidtbauer, "Modeling and control of variable-speed wind-turbine drive-system dynamics" *IEEE Control system magazine*, 15(4):28-38, August 1995.

[13] P. Schaak and T. G. van Engelen, "Torque control for variable speed wind turbines," *Proc. of the European Wind Energy Conf. - EWEC 2004*, UK, 2004.